Appendix A

Supplementary Material

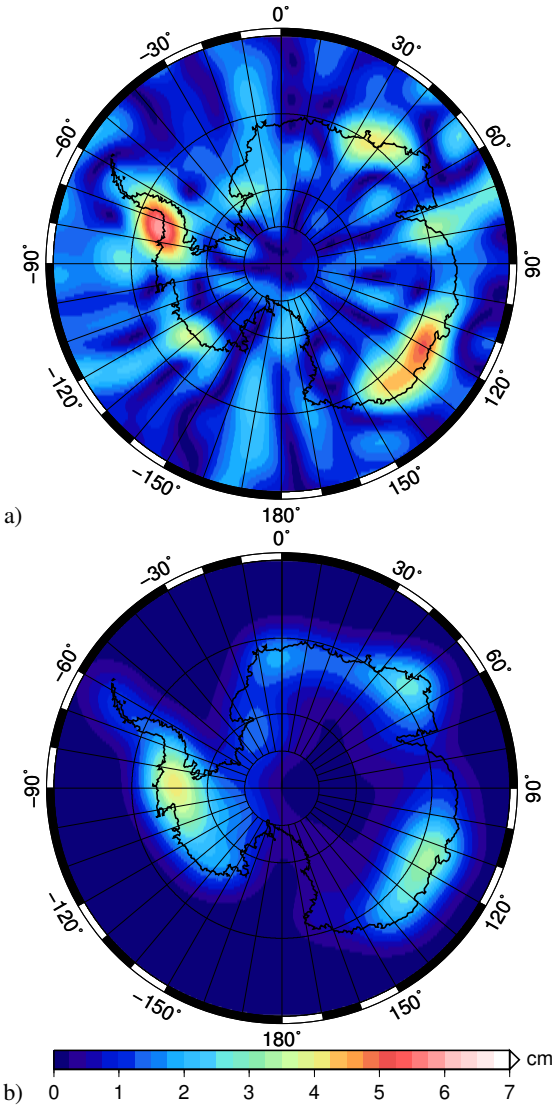

Fig. SM1. Magnitude of K2-periodic signal in EWH for a) GRACE CSR RL04 DDK3 and b) RACMO2 SMB.

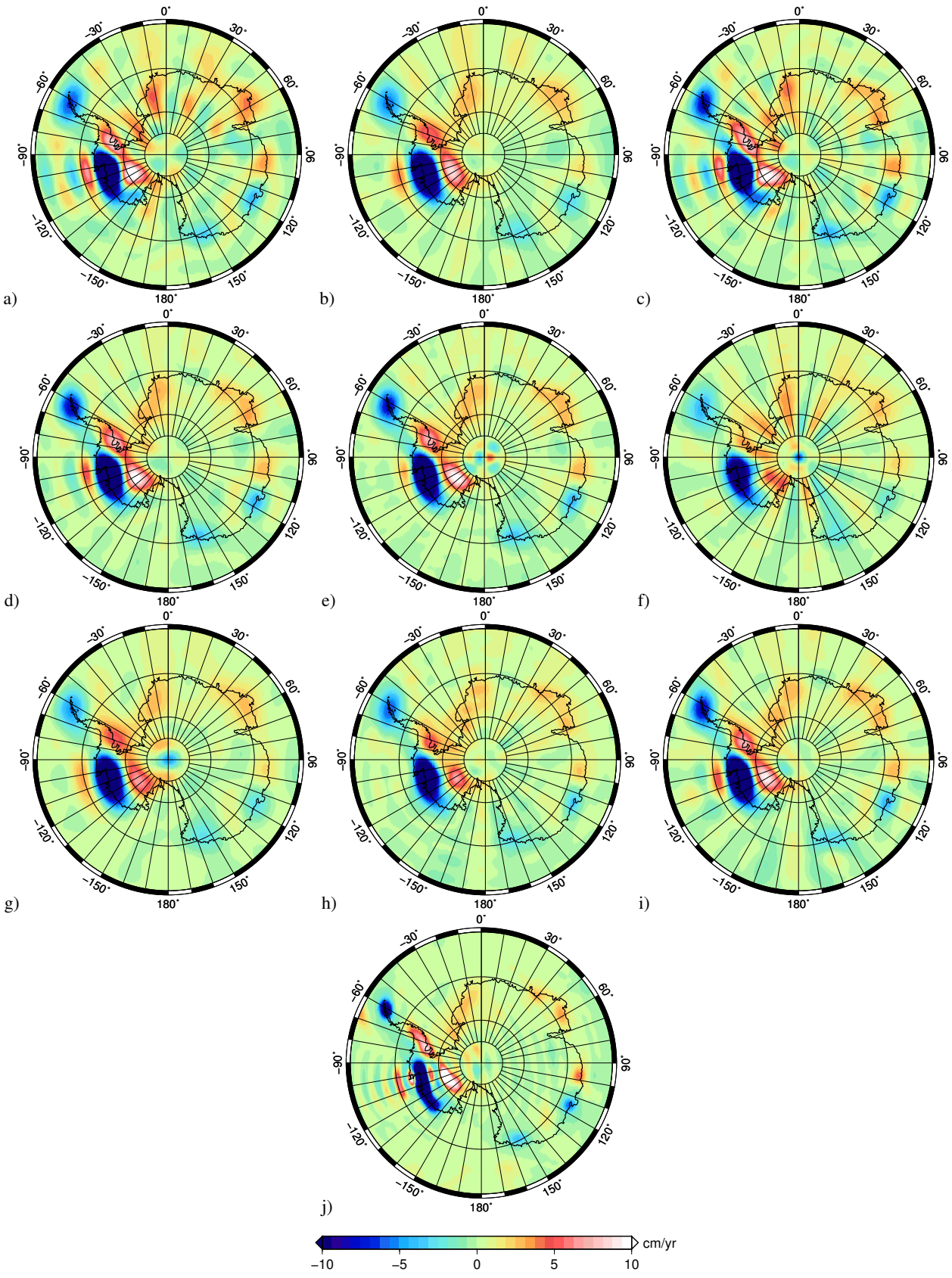

Fig. SM2. Mass change trends of the following GRACE solutions, in units of EWH: a) CSR RL04, b) CSR RL04 DDK3, c) CSR RL05, d) CSR RL05 DDK5, e) CSR RL05 Regularized, f) GFZ RL04, g) GFZ RL04 DDK3, h) GFZ RL05, i) GFZ RL05 DDK5, j) DMT-1b. For the plots shown, the unconstrained solutions (a, c, f, h) were de-striped before trend-fitting, and only the GFZ fields (f, h) have had an additional 200km Gaussian smoothing applied to improve visualization.

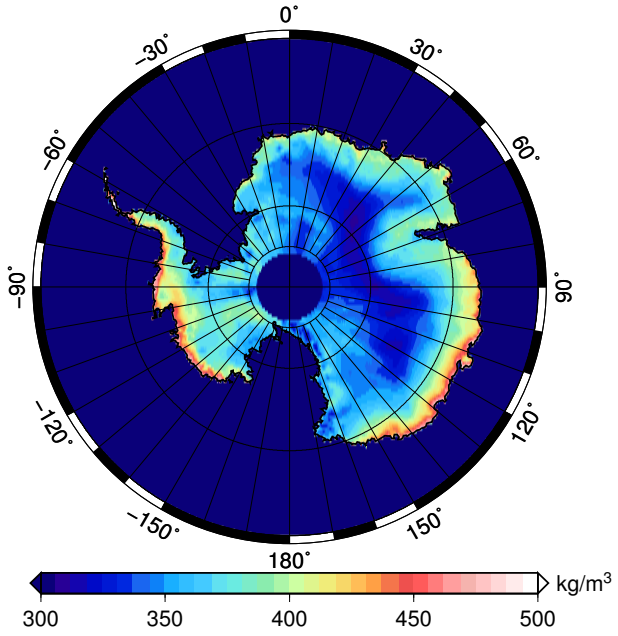

Fig. SM3. Surface density profile used to compute mass changes associated with differences between the FDM and altimetry surface heights.

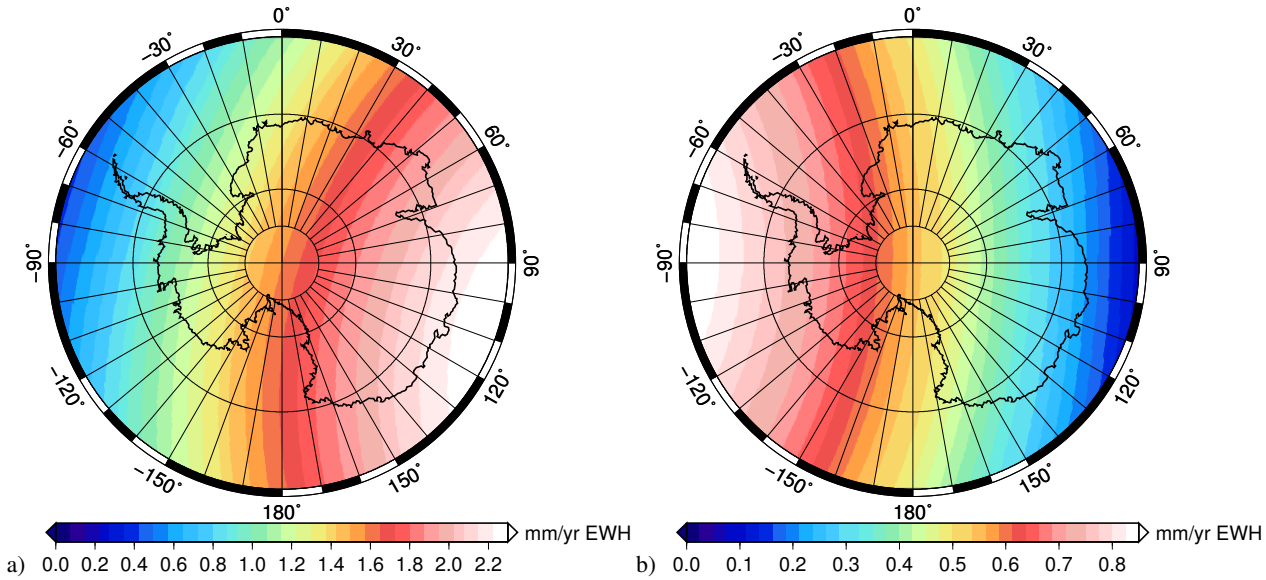

Fig. SM4. Comparison of degree one trends, in units of EWH, for two different sets of degree one coefficients: a) from Cheng et al (2011), and b) from Swenson et al (2008).

Table SM1. Influence of the two sets of degree one coefficients on the final solution estimates.

	LPZ bias		Total Est. Mass Change			Estimated GIA			Ice mass change		
	GIA	GRACE	from GRACE (Gt/yr)			(Gt/yr)			GRACE - GIA (Gt/yr)		
Solution	mm/yr	mm/yr EWH	EA	WA	AIS	EA	WA	AIS	EA	WA	AIS
CSR RL05 DDK5, deg1SW05	1.9	1.7	42	-78	-36	37	27	64	5	-105	-100
CSR RL05 DDK5, deg1SLR05	2.3	3.0	40	-83	-43	35	22	58	5	-105	-100

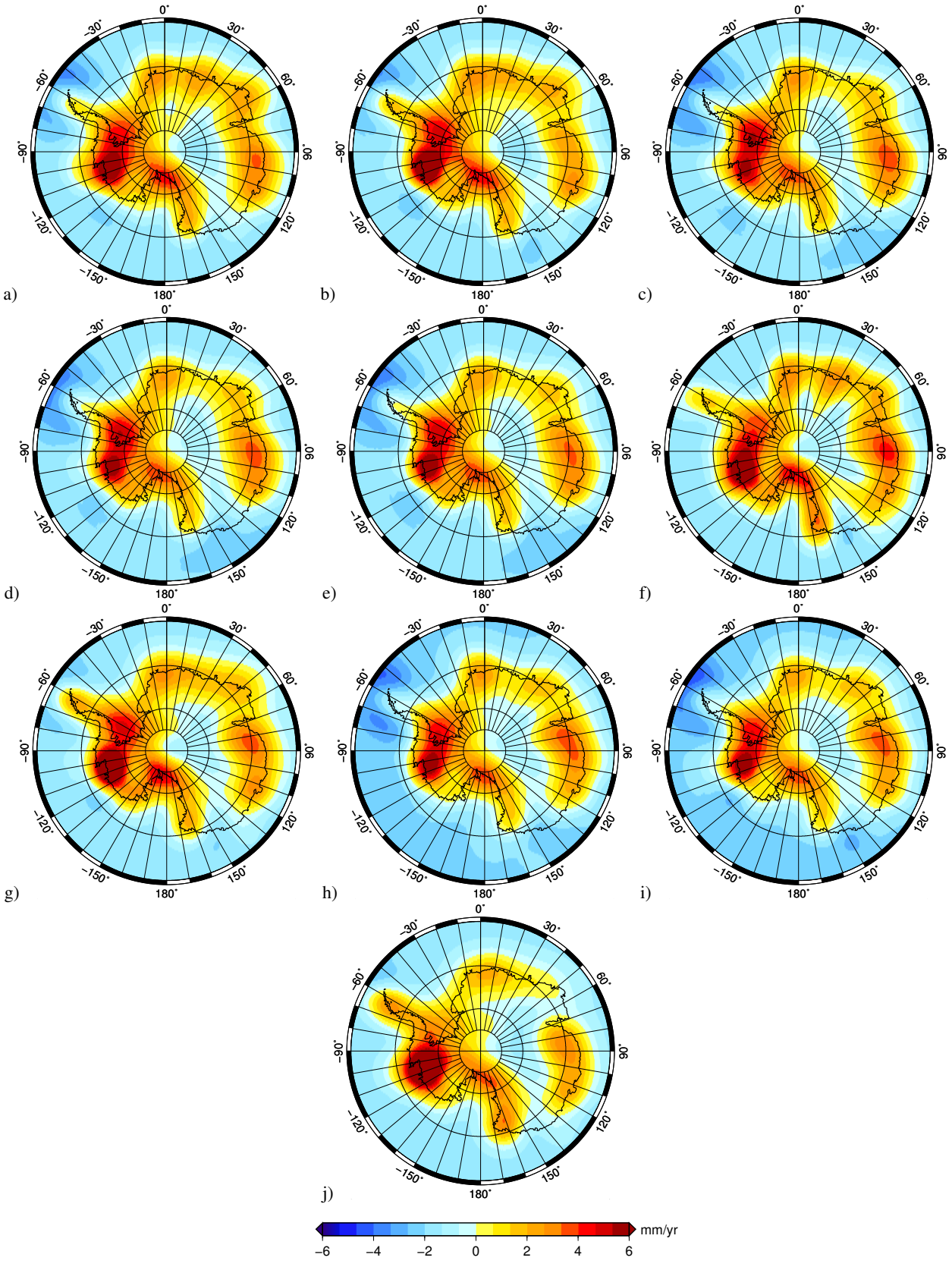

Fig. SM5. Estimated GIA vertical rates computed from the following GRACE solutions: a) CSR RL04, b) CSR RL04 DDK3, c) CSR RL05, d) CSR RL05 DDK5, e) CSR RL05 Regularized, f) GFZ RL04, g) GFZ RL04 DDK3, h) GFZ RL05, i) GFZ RL05 DDK5, j) DMT-1b

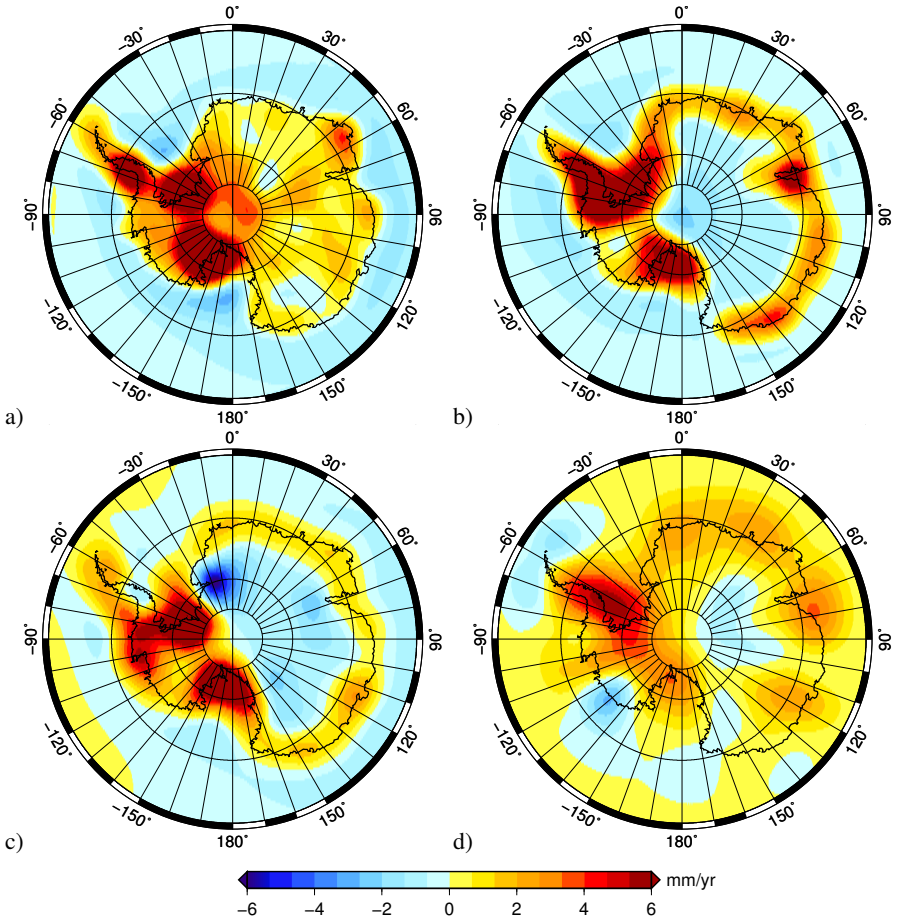

Fig. SM6. Original GIA uplift rates for a) ICE-5G, b) IJ05, and c) W12a, d) Riva09.